

NUMERICAL CALCULATION OF THE NEOCLASSICAL DISTRIBUTION FUNCTIONS AND CURRENT PROFILES

B.C. LYONS (PPPL), S.C. JARDIN (PPPL), J.J. RAMOS (MIT PSFC)

CEMM GROUP MEETING
MADISON, WI
TUESDAY, JUNE 12, 2012

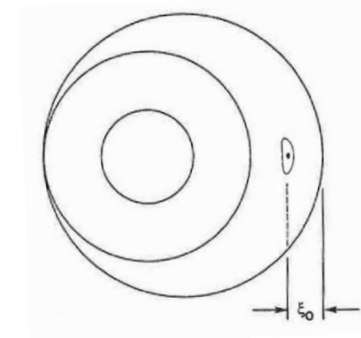
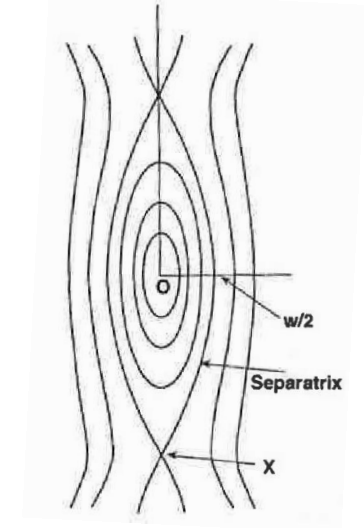
Acknowledgements

- This work has been supported by
 - ▣ the U.S. Department of Energy under grant nos. DEFC02-08ER54969 and DEAC02-09CH11466 and the SciDAC Center for Extended Magnetohydrodynamic Modeling (CEMM).
 - ▣ an award from the Department of Energy (DOE) Office of Science Graduate Fellowship Program (DOE SCGF). The DOE SCGF Program was made possible in part by the American Recovery and Reinvestment Act of 2009. The DOE SCGF program is administered by the Oak Ridge Institute for Science and Education for the DOE. ORISE is managed by Oak Ridge Associated Universities (ORAU) under DOE contract number DE-AC05-06OR23100. All opinions expressed in this presentation are the author's and do not necessarily reflect the policies and views of DOE, ORAU, or ORISE.

Neoclassical tearing mode (NTMs)

3

- Density, temperature, pressure, etc. tend to equilibrate across an island width
- Difference in current at O-point and X-point can drive island growth
 - ▣ Without these gradients, there can be no bootstrap current within the island
 - ▣ Bootstrap current at the X-point can drive island growth
- Large islands allow hot, dense plasma near core to be transported outward, reducing confinement
- Modifications to magnetic topology can result in macroscopic instability and disruption



Images taken from [The Theory of Toroidally Confined Plasmas](#) by R. White, 2006

NTM stability modeling

4

- NTM stability place a severe limit on maximum β
- Most common cause of disruptions on JET¹
- NTMs incorporate a lot of physics
 - ▣ Cause: Neoclassical kinetic theory
 - ▣ Effect: MHD destabilization
 - ▣ Requires a hybrid model
- High-fidelity simulations required for prediction, control, avoidance, and understanding of NTMs
 - ▣ Especially important for ITER operation, in which very few disruptions can be tolerated²

¹ P.C. de Vries, et al., Nucl. Fusion 51, 053018 (2011)

² T.C. Hender, et al., Nucl. Fusion 47, S128-S202 (2007)

Framework for hybrid solver

5

What's needed

Solve the drift kinetic equation in a **3D nonaxisymmetric**, toroidal geometry for the ion and electron perturbed distribution functions in parameter regimes **relevant to ITER and reactors** and **couple to an MHD solver**

Completed work

NIES- The Neoclassical Ion-Electron Solver

Solves the drift kinetic equation in a **2D axisymmetric tokamak** for the **neoclassical ion (simplified)** and electron perturbed distribution functions

Drift-Kinetic Equation

6

$$\frac{\partial \bar{f}_s}{\partial t} + \dot{\mathbf{x}} \cdot \frac{\partial \bar{f}_s}{\partial \mathbf{x}} + \dot{v}_{\parallel} \frac{\partial \bar{f}_s}{\partial v_{\parallel}} + \dot{v}_{\perp} \frac{\partial \bar{f}_s}{\partial v_{\perp}} = \langle C_{ss} [f_s, f_s] + C_{ss'} [f_s, f_{s'}] \rangle$$

- Collision operators taken in their linearized Landau form
- Velocity taken in frame of each species' macroscopic flow
- Two expansion parameters for high-temperature fusion plasmas

$$\delta \sim \rho_i / L \ll 1 \quad \nu_* \sim L / \lambda_{\text{mfp}} \sim \delta$$

- Maintain equations to lowest order exhibiting collisional dynamics
- Electron DKE is maintained to order $\delta_e \nu_*$, or δ^3
- Ion DKE should be maintained to order δ^2
- For now, ion DKE is maintained to order $\delta \nu_*$
- This is conventional neoclassical banana dynamics for both species
- Assume stationary, axisymmetric equilibria

Resulting DKE

7

- Given these assumptions, it is convenient to write

$$\bar{f}_s = (1 + g_{s,0} + g_{s,1} v_{\parallel}) f_{Ms} + h_s$$

where $g_{s,0}$ and $g_{s,1}$ have analytic forms

- Then, the DKE for h_s can be reduced to

$$v_{\parallel} (\mathbf{b} \cdot \nabla \theta) \frac{\partial h_s}{\partial \theta} - C_s [h_s] = S_s v_{\parallel} \quad \star$$

where $v_{\parallel}(\psi, \theta, v, \lambda) = \pm v [1 - \lambda B(\psi, \theta) / B_{max}(\psi)]^{1/2}$

$$\lambda(\psi, \theta, \chi) = \sin^2 \chi B_{max}(\psi) / B(\psi, \theta)$$

★ We'll come back to this form later

Source Terms

8

- Electron source contains Ohmic drive, interaction with ion flow, and pressure and temperature gradient bootstrap drive

$$S_e = \left\{ \frac{eV_{loop}I}{2\pi T_e B R^2} + \nu_e \left(U_i B + \frac{I}{enB} \frac{dP}{d\psi} \right) \frac{v_{the}}{v_{thi}^2 v} \xi \left(\frac{v}{v_{thi}} \right) \right. \\ \left. + \frac{\nu_e m_e I}{e B T_e} \frac{dT_e}{d\psi} \frac{v_{the}}{v} \left[2\varphi \left(\frac{v}{v_{the}} \right) - 10\xi \left(\frac{v}{v_{the}} \right) \right. \right. \\ \left. \left. + \frac{1}{2} \varphi \left(\frac{v}{v_{thi}} \right) - \frac{5v_{the}^2}{2v_{thi}^2} \xi \left(\frac{v}{v_{thi}} \right) \right] \right\} f_{Me}$$

- Ion source has only temperature gradient drive

Solvability Condition

9

- Standard solution method for neoclassical theory

$$h_s = \underbrace{\zeta(v_{\parallel})H(1 - \lambda)K_s(\psi, v, \lambda)}_{h^{odd}} + h_s^{even}(\psi, \theta, v, \lambda)$$

- DKE becomes $v_{\parallel}(\mathbf{b} \cdot \nabla\theta) \frac{\partial h_s^{even}}{\partial \theta} - C_s [\zeta H K_s] = S_s v_{\parallel}$

- Solvability condition: $\oint_{\psi, v, \lambda} \frac{dl}{v_{\parallel}} C_s [\zeta H K_s] = - \oint_{\psi, v, \lambda} dl S_s$

- Contour integrals taken along one poloidal turn of magnetic field line

Integral over Collision Operator

10

$$\begin{aligned}
 \oint_{\psi, v, \lambda} \frac{dl}{v_{\parallel}} C_e[h^{odd}] = & \frac{2\nu_D}{v} \frac{\partial}{\partial \lambda} \left(\eta_1 \lambda \frac{\partial}{\partial \lambda} K_e \right) \\
 & + \nu_e \eta_2 v_{the}^3 \left[\frac{1}{v^3} \frac{d}{dv} \left\{ \begin{aligned} & \xi \left(\frac{v}{v_{the}} \right) \left[v \frac{d}{dv} + \frac{v^2}{v_{the}^2} \right] \\ & + \xi \left(\frac{v}{v_{thi}} \right) \left[v \frac{d}{dv} + \frac{m_e v^2}{m_i v_{thi}^2} \right] \end{aligned} \right\} + \frac{4\pi f_{Me}}{nv} \right] K_e \\
 & - \frac{\nu_e v_{the}}{nv} f_{Me} \int_0^{2\pi} JB \left[1 - \lambda \frac{B}{B_{max}} \right]^{-\frac{1}{2}} \Phi d\theta \\
 & + \frac{\nu_e v}{nv_{the}} f_{Me} \frac{d^2}{dv^2} \int_0^{2\pi} JB \left[1 - \lambda \frac{B}{B_{max}} \right]^{-\frac{1}{2}} \Psi d\theta
 \end{aligned}$$

where

$$\eta_1(\psi, \lambda) = B_{max} \int_0^{2\pi} J \left[1 - \lambda \frac{B}{B_{max}} \right]^{\frac{1}{2}} d\theta$$

$$\eta_2(\psi, \lambda) = \int_0^{2\pi} JB \left[1 - \lambda \frac{B}{B_{max}} \right]^{-\frac{1}{2}} d\theta$$

Expansions

- Expand Rosenbluth Potentials in Legendre and Fourier series

$$\begin{pmatrix} \Phi_s \\ \Psi_s \end{pmatrix} = \sum_{m=0}^M \sum_{l=1, \text{odd}}^{2L-1} \begin{pmatrix} \Phi_s^{l,m}(v) \\ \Psi_s^{l,m}(v) \end{pmatrix} P_l(y) \cos m\theta$$

- Then expand K_s , $\Phi_s^{l,m}$, and $\Psi_s^{l,m}$ in finite elements in v and λ , as necessary

$$K_s(v, \lambda) = \sum_{i=0}^N \sum_{j=0}^J K_s^{i,j} \phi_i(v) \phi_j(\lambda)$$

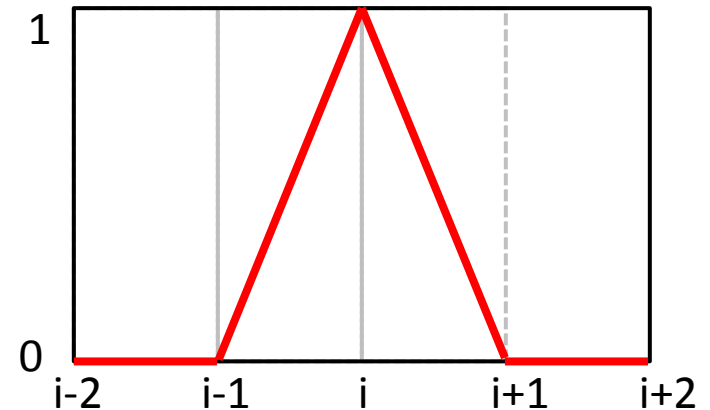
$$\begin{pmatrix} \Phi_s^q(v) \\ \Psi_s^q(v) \end{pmatrix} = \sum_{i=0}^N \begin{pmatrix} \Phi_s^{i,q} \\ \Psi_s^{i,q} \end{pmatrix} \phi_i(v)$$

Galerkin Method

12

- Take the inner product of the previous equations with each finite element
- Use linear tent functions:
- Only overlap with their two nearest neighbors and themselves
- DKE becomes tridiagonal in both v and λ
- Rosenbluth Potential eqs. are tridiagonal in v and dense in λ

$$\varphi_p(x) = \begin{cases} \frac{x-x_{i-1}}{x_i-x_{i-1}} & : x_{i-1} \leq x \leq x_i \\ \frac{x_{i+1}-x}{x_{i+1}-x_i} & : x_i \leq x \leq x_{i+1} \end{cases}$$



Block Tridiagonal Algorithm

13

- Since all equations are tridiagonal in v , we rewrite the coupled set as a block tridiagonal matrix eq.

$$\mathbf{A}_i \cdot \mathbf{U}_{i+1} - \mathbf{B}_i \cdot \mathbf{U}_i + \mathbf{C}_i \cdot \mathbf{U}_{i-1} = \mathbf{D}_i$$

- Size of each block matrix is $(J + 2L(M + 1))^2$
- Given appropriate boundary conditions, there exists a straightforward algorithm to solve for \mathbf{U}
- Computation time required is $O(N (J + 2L(M + 1))^3)$

Boundary Conditions

14

□ For v

$$\square K_s(0, \lambda) = 0 \quad K_s(" \infty " = v_{max}, \lambda) = 0$$

$$\square \Phi_{l,m}(0) = 0 \quad \frac{d\Phi_{l,m}}{dv}(v_{max}) = -(l+1) \frac{\Phi_{l,m}(v_{max})}{v_{max}}$$

$$\square \Psi_{l,m}(0) = 0 \quad \frac{d\Psi_{l,m}}{dv}(v_{max}) = -(l-1) \frac{\Psi_{l,m}(v_{max})}{v_{max}}$$

□ For λ

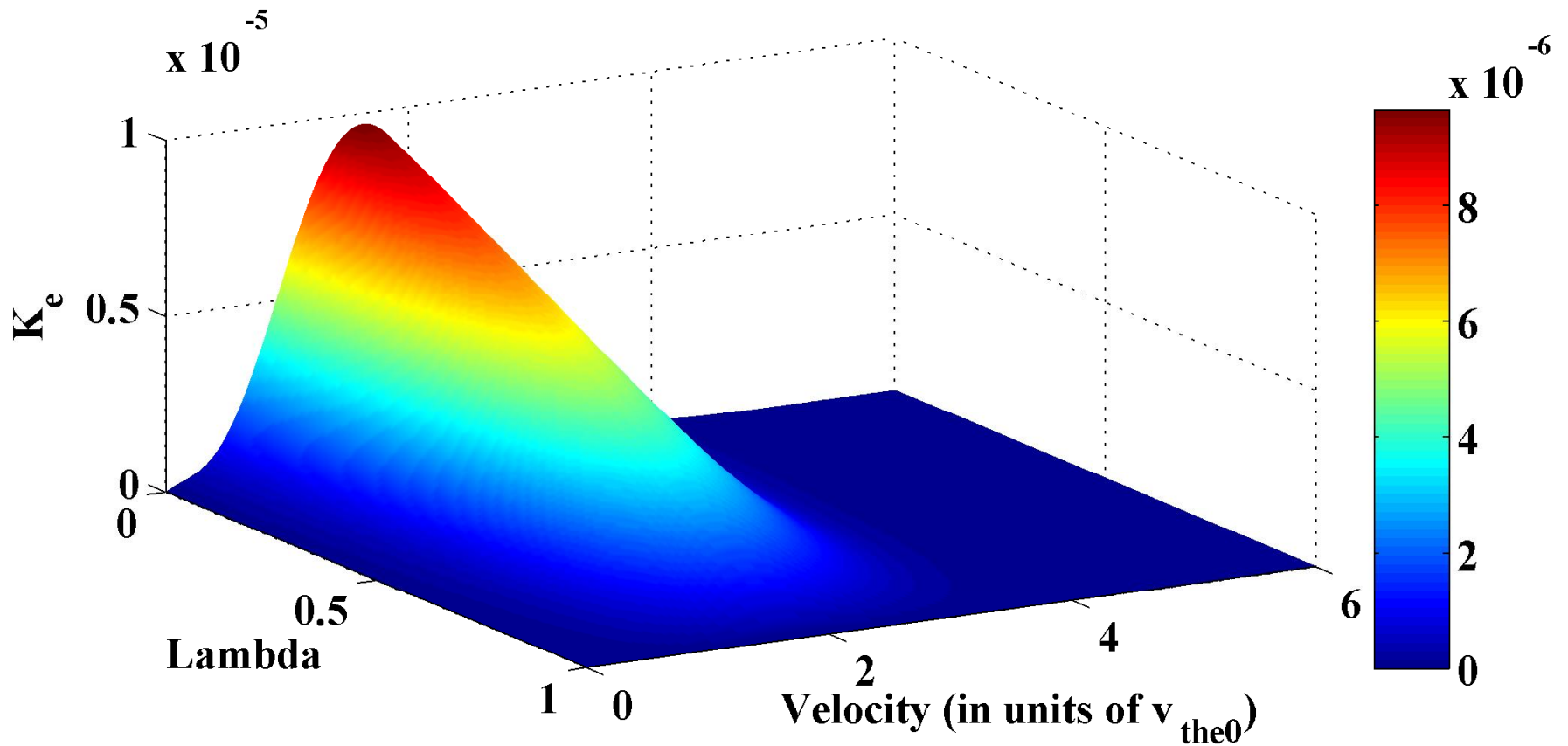
$$\square \lim_{\lambda \rightarrow 0} \lambda^{1/2} \frac{\partial K_s(v, \lambda)}{\partial \lambda} = 0$$

$$\square K_s(v, 1) = 0$$

$$\square \frac{\partial K_s}{\partial \lambda}(v, 1) = 0 \quad \text{requires boundary layer}$$

Example Distribution Functions (1)

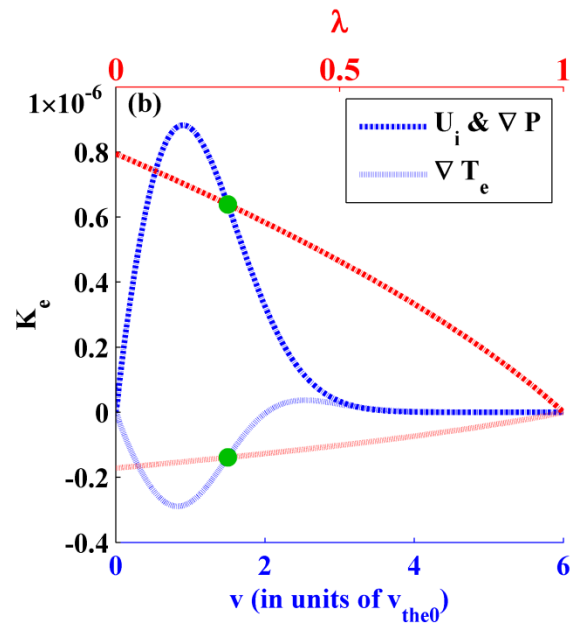
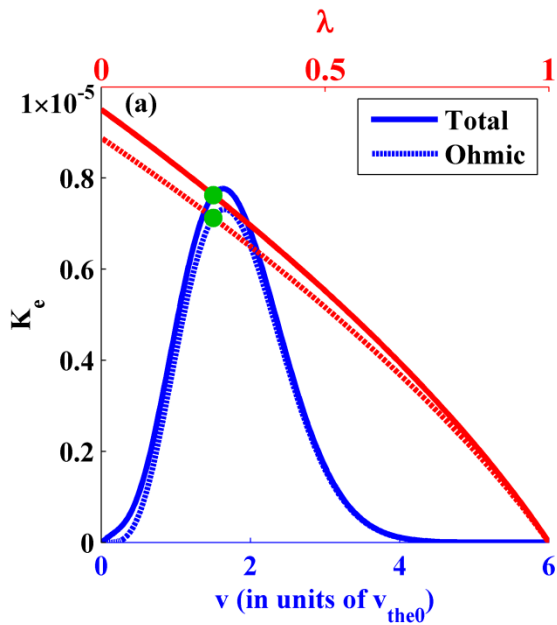
15



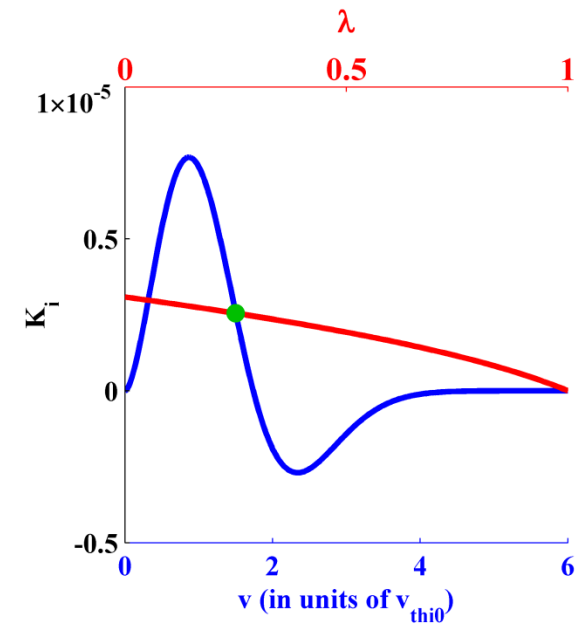
Example Distribution Functions (2)

16

Electrons

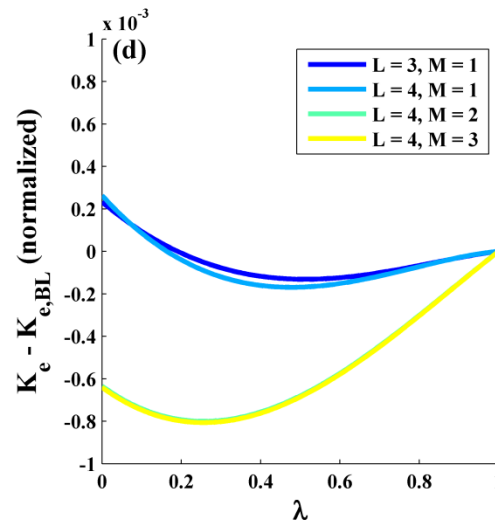
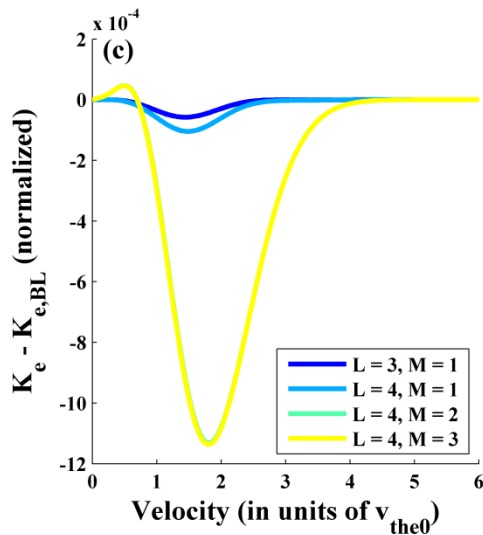
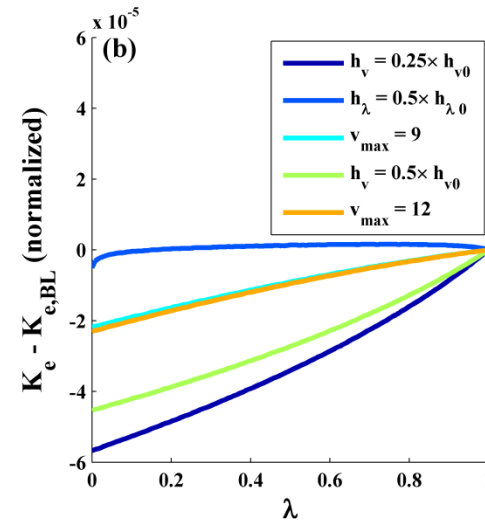
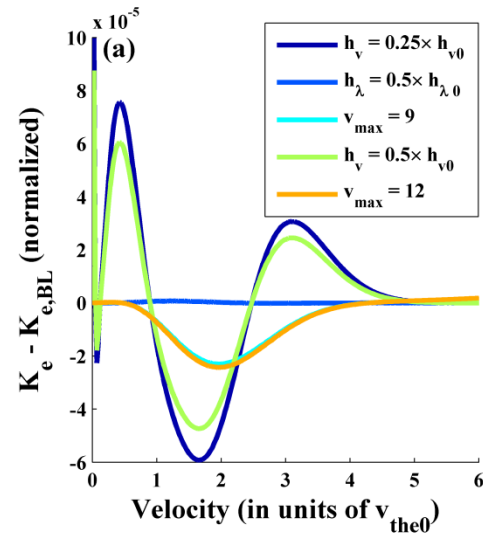


Ions



Convergence

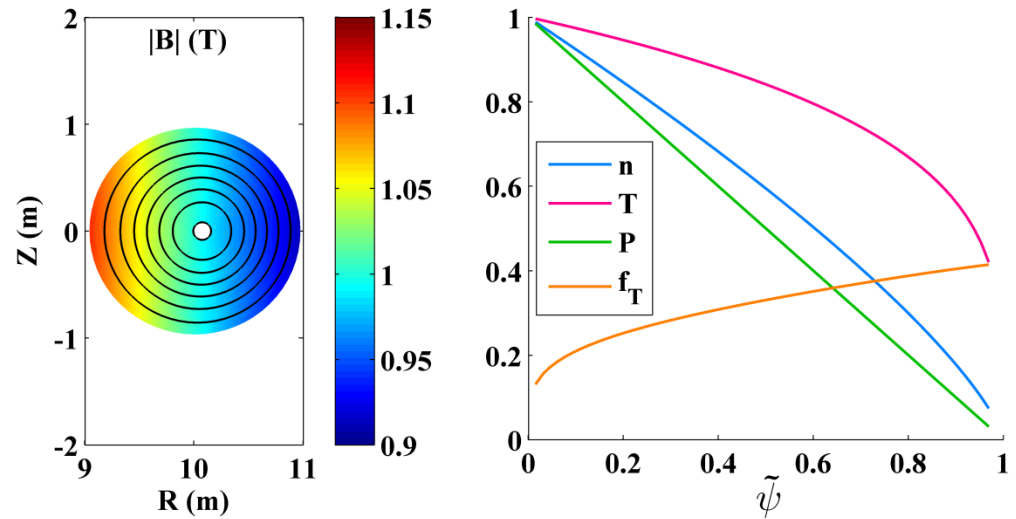
17



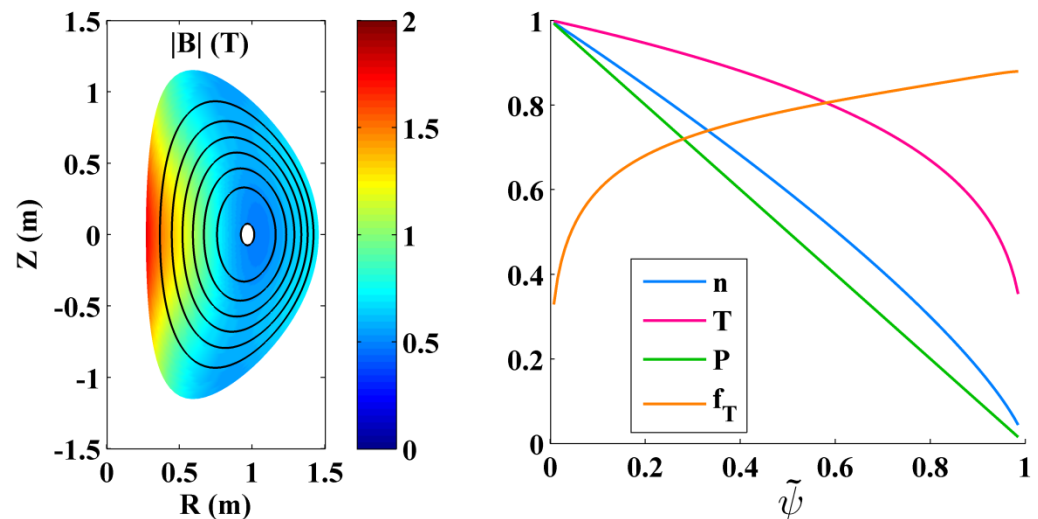
JSOLVER Equilibria Used

18

Large Aspect Ratio



NSTX

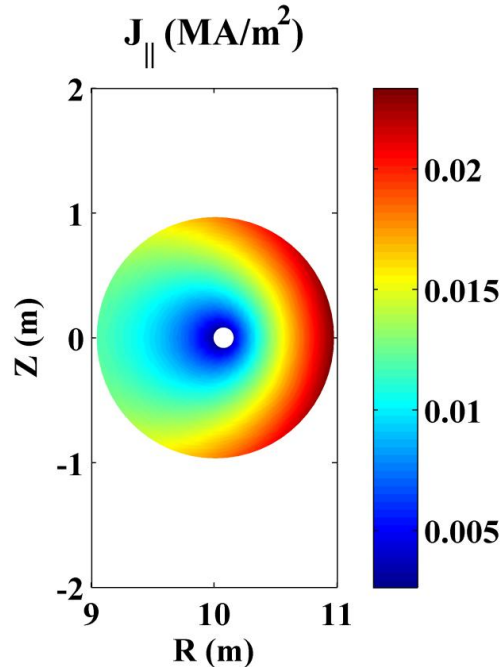


Calculating Current

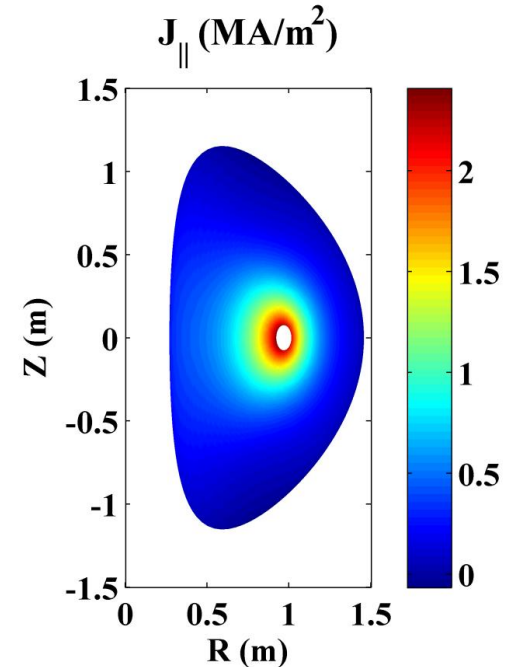
19

- One can show that
$$U_s(\psi) = \frac{2\pi}{nB_{max}} \int_0^\infty dv v^3 \int_0^1 d\lambda K_s(\psi, v, \lambda)$$
- Current can be calculated from
$$j_{\parallel} = (U_i - U_e)B + \frac{I}{B} \frac{dP}{d\psi}$$

Large Aspect
Ratio



NSTX



Sauter Analytic Fits [(1999) Phys. Plasmas: 6,7]

20

- Fits numerical solutions for a wide variety of equilibria

$$\langle J_{\parallel} B \rangle = \sigma_{neo} \langle E_{\parallel} B \rangle - I(\psi) \left[\mathcal{L}_{31} \frac{\partial p}{\partial \Psi} + \mathcal{L}_{32} n_e \frac{\partial T_e}{\partial \Psi} + \mathcal{L}_{34} \alpha n_i \frac{\partial T_i}{\partial \Psi} \right]$$

$$\frac{\sigma_{neo}}{\sigma_{Sptz}} = 1 - 1.36 f_t + 0.59 f_t^2 - 0.23 f_t^3$$

$$\mathcal{L}_{31} = \mathcal{L}_{34} = 1.7 f_t - 0.95 f_t^2 + 0.15 f_t^3 + 0.1 f_t^4$$

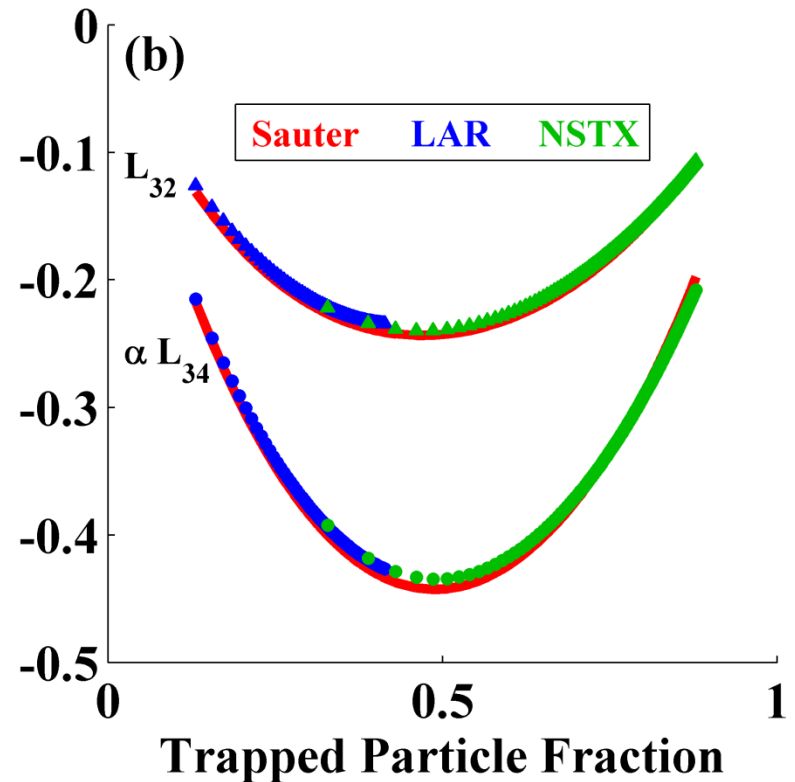
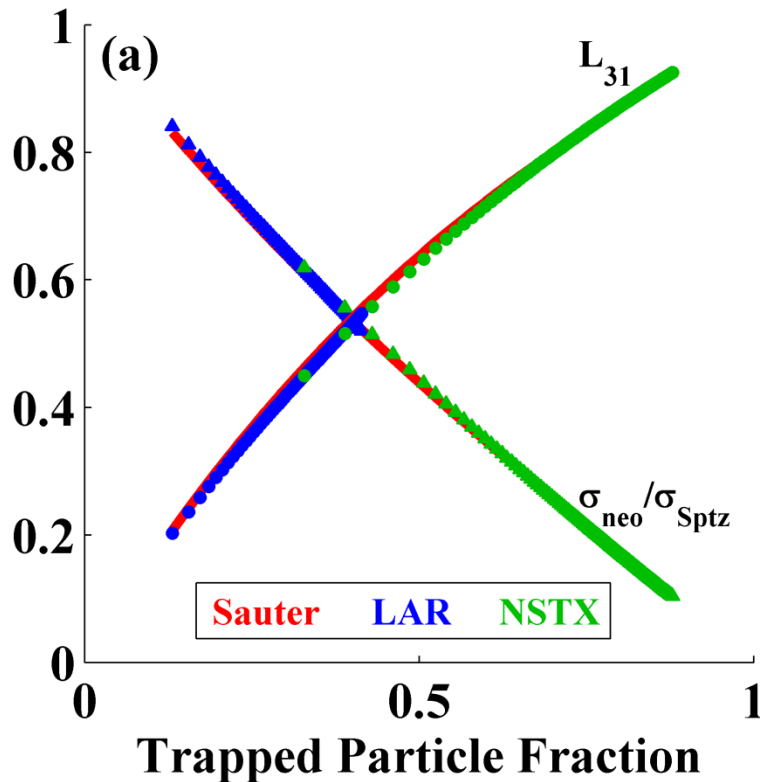
$$\mathcal{L}_{32} = -1.26(f_t - f_t^4) + 2.24(f_t^2 - f_t^4) - 1.77(f_t^3 - f_t^4)$$

$$\alpha = -\frac{1.17(1 - f_t)}{1 - 0.22 f_t - 0.19 f_t^2}$$

where $f_t = 1 - \frac{3}{4} \left\langle \frac{B^2}{B_{max}^2} \right\rangle \int_0^1 \frac{\lambda d\lambda}{\left\langle \sqrt{1 - \lambda B / B_{max}} \right\rangle}$

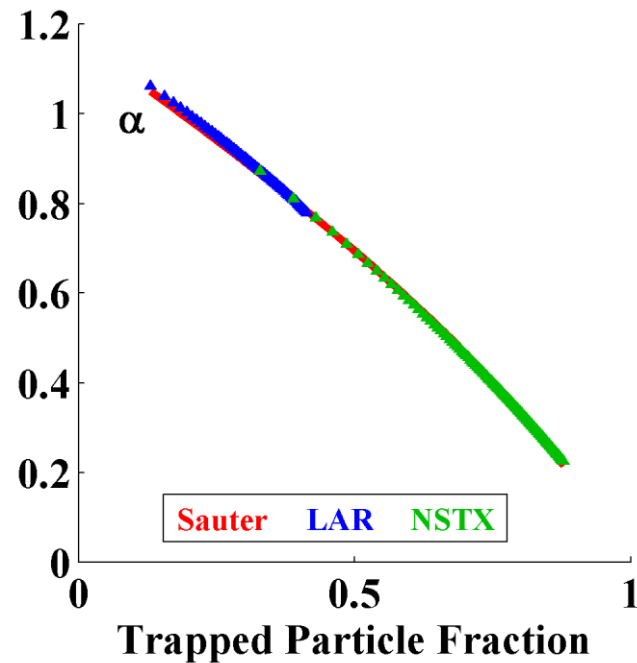
Bootstrap Current Coefficients

21



Ion Flow Coefficient

22



where
$$U_i = \alpha \frac{cI}{e \langle B^2 \rangle} \frac{dT_i}{d\psi}$$

Summary of Completed Work

23

- A code has been written to solve for the component of the non-Maxwellian ion and electron distribution functions necessary to compute the current in an axisymmetric toroidal plasma
- Results for all sources have been benchmarked against the Sauter analytic fits

Future Work

24

- Calculate radial fluxes (See Jesus's talk to follow)
- Allow distribution function to vary poloidally
- Generalize to 3D Geometry
- Develop ion theory to appropriate ordering
- Implement fully 3D, coupled ion-electron code
- Couple with MHD code (e.g., M3D-C1)
- Perform NTM and sawtooth studies

Towards a Nonaxisymmetric Code

25

- The spatially 3D drift-kinetic equation is quite complex, even to first-order in δ_s

$$\begin{aligned}
 & \frac{\partial \bar{f}_{NMe}}{\partial t} + \cos \chi \left(v' \mathbf{b} \cdot \frac{\partial \bar{f}_{NMe}}{\partial \mathbf{x}} + v_{the}^2 \mathbf{b} \cdot \nabla \ln n \frac{\partial \bar{f}_{NMe}}{\partial v'} \right) - \frac{\sin \chi}{v'} \left(v_{the}^2 \mathbf{b} \cdot \nabla \ln n - \frac{v'^2}{2} \mathbf{b} \cdot \nabla \ln B \right) \frac{\partial \bar{f}_{NMe}}{\partial \chi} \\
 & = \left\{ \cos \chi \frac{v'}{2T_e} \left(5 - \frac{v'^2}{v_{the}^2} \right) \mathbf{b} \cdot \nabla T_e + \cos \chi \frac{v'}{nT_e} \mathbf{b} \cdot \left[\frac{2}{3} \nabla (p_{e\parallel} - p_{e\perp}) - (p_{e\parallel} - p_{e\perp}) \nabla \ln B - \mathbf{F}_e^{\text{coll}} \right] \right. \\
 & \quad + P_2(\cos \chi) \frac{v'^2}{3v_{the}^2} (\nabla \cdot \mathbf{u}_e - 3\mathbf{b} \cdot [(\mathbf{b} \cdot \nabla) \mathbf{u}_e]) + \frac{1}{3nT_e} \left(\frac{v'^2}{v_{the}^2} - 3 \right) [\nabla \cdot (q_{e\parallel} \mathbf{b}) - G_e^{\text{coll}}] \\
 & \quad + \frac{1}{6eB} \left[2P_2(\cos \chi) \frac{v'^2}{v_{the}^2} \left(\frac{v'^2}{v_{the}^2} - 5 \right) + \frac{v'^4}{v_{the}^4} - 10 \frac{v'^2}{v_{the}^2} + 15 \right] (\mathbf{b} \times \boldsymbol{\kappa}) \cdot \nabla T_e \\
 & \quad + \frac{1}{6eB} \left[-P_2(\cos \chi) \frac{v'^2}{v_{the}^2} \left(\frac{v'^2}{v_{the}^2} - 5 \right) + \frac{v'^4}{v_{the}^4} - 10 \frac{v'^2}{v_{the}^2} + 15 \right] (\mathbf{b} \times \nabla \ln B) \cdot \nabla T_e \\
 & \quad \left. + P_2(\cos \chi) \frac{v'^2}{3eBv_{the}^2} (\mathbf{b} \times \nabla \ln n) \cdot \nabla T_e \right\} f_{Me} + \langle C_{ee}[f_e, f_e] + C_{ei}[f_e, f_i] \rangle_\alpha,
 \end{aligned}$$

Path 1 – Build Up From Existing Code

26

- Currently we calculate lowest order collisionality distribution function (constant on flux surface)
- Instead of using the solvability condition, we can solve the 3D (i.e., 1 spatial + 2 velocity) equation

$$v_{\parallel} (\mathbf{b} \cdot \nabla \theta) \frac{\partial h_s}{\partial \theta} - C_s [h_s] = S_s v_{\parallel}$$

- New expansions
 - ▣ h_s , Φ_s , and Ψ_s in Fourier series in both sines and cosines
 - ▣ h_s in finite elements in $\cos \chi$ (BCs in λ too difficult)

Pros/Cons of Path 1

27

- Advantages
 - ▣ Relatively simple: code is largely the same
 - ▣ Extends current code to higher collisionality
- Disadvantages
 - ▣ Several codes already do something like this, typically with more features (e.g., NEO, CQLP)
 - ▣ It is unclear what we would learn from this step that could be directly applied to the spatially 3D equation

Path 2 – Start Working on 3D Eq.

28

- First look at largest terms in the spatially 3D eq.

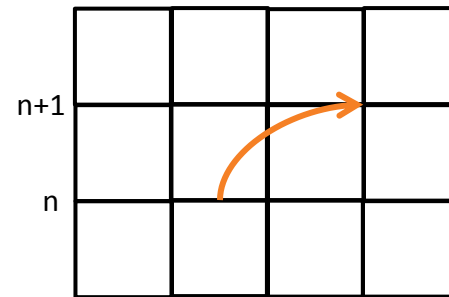
$$\frac{\partial \bar{f}_{NM_s}}{\partial t} + \cos \chi \left(v \mathbf{b} \cdot \frac{\partial \bar{f}_{NM_s}}{\partial \mathbf{x}} + v_{ths}^2 \mathbf{b} \cdot \nabla \ln n \frac{\partial \bar{f}_{NM_s}}{\partial v} \right) - \frac{\sin \chi}{v} \left(v_{ths}^2 \mathbf{b} \cdot \nabla \ln n - \frac{v^2}{2} \mathbf{b} \cdot \nabla \ln B \right) \frac{\partial \bar{f}_{NM_s}}{\partial \chi} = 0$$

- Further assume a small parallel density gradient
- Requires only balancing three terms

Possible Solution Method

29

- Iterative solution to steady-state for given equilibrium
- Semi-Lagrangian method*
 - Implicit algorithm
 - Method of characteristics for convective terms
 - Requires high-order interpolation at time step n
 - Operator splitting to handle all other terms
- Use M3D-C1 finite elements
 - High-order basis elements already provide necessary interpolation
 - Allows for easy integration with the M3D-C1 code



* E. Sonnendrücker, ICNSP 2011; C.Z. Cheng and G. Knorr, J. Comp. Phys. 22, 330-351 (1976).

Pros/Cons of Path 2

30

- Advantages
 - ▣ Directly applicable to full nonaxisymmetric code
 - ▣ Provides experience working w/ 3D fields and meshes
 - ▣ Simple checks
 - μ conservation
 - If collision operator is included, should provide identical results to Path 1 (assuming axisymmetric field is given)
- Disadvantages
 - ▣ Will require careful development of algorithm
 - ▣ Too big of a step?

Conclusion

31

- Work thus far has been promising
- Still a long way to go
- Likely path forward is along both Paths 1 & 2
 - ▣ Any thoughts on those paths?